Electrochemical Characterization of (ZnO/dsDNA)$_n$ Layer-by-layer Films and Detection of Natural DNA Oxidative Damage

DU, Meng(杜萌)   YANG, Tao(杨涛)   ZHANG, Yongchun(张永春)   JIAO, Kui*(焦奎)

Key Laboratory of Eco-chemical Engineering (*Ministry of Education*), *College of Chemistry and Molecular Engineering*, *Qingdao University of Science and Technology*, *Qingdao, Shandong 266042, China*

The positively charged nano-ZnO and negatively charged natural DNA were alternately adsorbed on the surface of a gold electrode, forming (ZnO/dsDNA)$_n$ layer-by-layer films. Valuable dynamic information for controlling the formation and growth of the films was obtained by cyclic voltammetry and electrochemical impedance spectroscopy. Differential pulse voltammetric (DPV) measurements showed that the electroactive probe methylene blue (MB) could be loaded in the (ZnO/dsDNA)$_n$ films from its solution, and then released from the films into Britton-Robinson (B-R) buffer. The complete reloading of MB in the films could be realized by immersing the films in MB solution again. However, after incubation in the solution of carcinogenic metal nickel, the damaged (ZnO/dsDNA)$_n$ films could not return to their original and fully-loaded state, and showed smaller DPV peak currents. The results demonstrated that the DNA damage induced by the hydroxyl radical could be achieved by electrochemistry.

Keywords   layer-by-layer, DNA damage, nano-ZnO, carcinogenic metal, nickel

Introduction

As a simple and versatile technique for fabricating ultrathin films on solid substrates, layer-by-layer assembly has aroused great interests in recent years,[1-3] which originates from the alternate adsorption of oppositely charged polyelectrolytes on solid surface from their solutions by electrostatic interaction.[4] One of the distinguished advantages of layer-by-layer assembly over casting and dip-coating methods is that the layer composition and thickness can be precisely tailored by controlling the type of charged species and the number of adsorption cycles according to a predesigned architecture. Unlike other molecularly controlled methods, such as self-assembly monolayers (SAM) and Langmuir-Blodgett membrane, the layer-by-layer assembly is very simple and versatile, and suitable to a variety of shapes of solid substrates. Nowadays, this technique has been extended to fabricate protein films, and various (protein/polyelectrolyte)$_n$ films have been successfully assembled.[5-8] This layer-by-layer method has also been applied to DNA assembly. For example, Wang *et al.*[9] have fabricated poly(dimethyldiallylammonium chloride) (PDDA) and DNA multilayer films by electrostatic layer-by-layer adsorption. Real-time surface plasmon resonance (SPR) technique was used to monitor layer-by-layer assembly of multilayer films in real time in solution continuously. The results showed that the uniform DNA/PDDA multilayer could be fabricated on poly(ethylenimine)- (PEI-) coated sensor chip surface and the precise control of the thickness of each layer in multilayer film could be realized by selecting the proper concentration and injection time of DNA and PDDA alternately.

ZnO is a very attractive semiconductor material. Bulk ZnO is widely used in rubber products, ceramics, paints, pharmaceuticals, and sensors.[10-12] Topoglidis and coworkers[13] reported the immobilization and bioelectrochemistry of proteins on nanoporous TiO$_2$ and ZnO films, and they suggested that ZnO with a high isoelectric point (*ca*. 9.5) was suitable for the adsorption of low-isoelectric point protein. Therefore, nano-ZnO deserves to be further investigated as an important promising candidate for the supporting material in the fabrication of biosensors.

In living systems, DNA damage is generally considered to be linked to senescence, neurological and tumor formation. Reactive oxygen species (ROS) are regarded as main DNA oxidative damage reagents. Guanine is the most easily oxidized DNA base, mainly producing 8-oxoguanine (8-oxoG). Damage to DNA also has the effect of unwinding the double helix.[14] In virtue of the redox reactions happening in the oxidative damage to DNA, some groups have developed several electrochemical biosensors for evaluating DNA damage.[15-17]
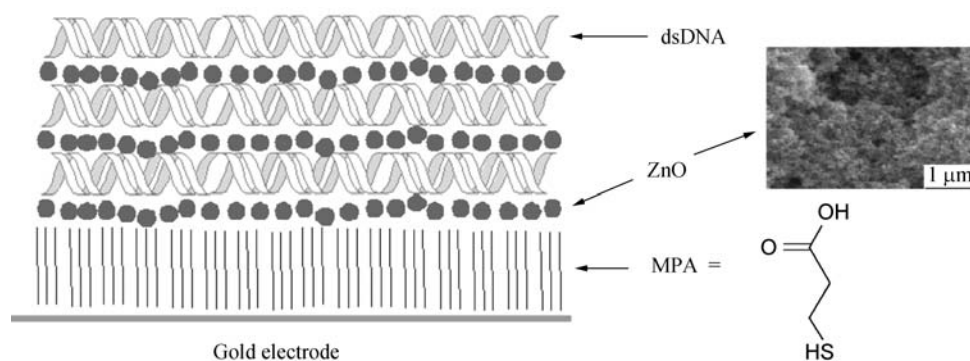
Figure 1 Scheme of the sequential self-assembly of the (ZnO/dsDNA)$_n$ multilayer.

In this work, layer-by-layer films of negatively charged natural DNA and positively charged nano-ZnO were firstly assembled on the 3-mercaptopropionic acid (MPA)-modified gold electrode surface (Figure 1 for the scheme of the build-up process). The assemblies were characterized by cyclic voltammetry (CV) and electrochemical impedance spectroscopy (EIS). Methylene blue (MB) was loaded in the films as an electroactive probe to detect the damage of DNA. NiSO$_4$ was chosen as the model damage agent for natural DNA. Differential pulse voltammetric (DPV) measurement of the loaded MB was used to detect dsDNA lesion at different exposure time of DNA layer-by-layer films in NiSO$_4$ solution. Compared with the intact DNA films, the damaged DNA films showed an obvious decrease in DPV peak currents for the loaded MB. The interactions of MB with dsDNA were also investigated in the presence and absence of Ni(II). We thus expected that the specific intercalation of MB into dsDNA base pairs and the different binding amounts of MB in intact and damaged dsDNA might provide a method for electrochemically detecting the DNA damage.

Experimental

Apparatus and reagents

A CHI 660C electrochemical analyzer (Shanghai CH Instrument Company, China), which was in connection with a gold modified working electrode, a Ag/AgCl reference electrode and a platinum wire auxiliary electrode, was used for the electrochemical measurements. The pH values of all solutions were measured by a model pHs-25 digital acidometer (Shanghai Leici Factory, China). Ultrapure water was prepared by aquapro ultrapure water system (Chongqing Yiyang Company, China).

Nano-ZnO (20—30 nm, scanning electron micrograph in Figure 1) was provided by College of Materials Science and Engineering, Qingdao University of Science and Technology; native double-stranded fish sperm DNA (dsDNA) was purchased from Beijing Jingke Reagent Company; MPA and MB were purchased from Sigma (St. Louis, MO, USA) and Shanghai Reagent Company (China), respectively. All the chemicals were of analytical grade and solutions were prepared with ultrapure water.

Procedures

The gold electrode was cleaned by immersing it in a 3 : 1 (*V* : *V*) mixture of concentrated sulfuric acid and 30% hydrogen peroxide (piranha solution) for about 5 min, followed by washing it thoroughly with ultrapure water. Then the electrode was polished on 0.3 and 0.05 μm α-Al$_2$O$_3$ pastes, respectively, followed by sonication in ultrapure water for 10 min. Finally, the electrode was cleaned electrochemically by cycling between -0.4 and 1.5 V versus Ag/AgCl in a 0.02 mol/L H$_2$SO$_4$ solution at a scan rate of 100 mV/s until reproducible cyclic voltammograms at a clean gold electrode were obtained. The electrode was immersed into an ethanol solution (5 mmol/L) of MPA for 12 h to obtain a self-assembly layer on the surface. The negatively charged MPA self-assembly layer was the anchor for the electrostatic adsorption of the positively charged ZnO (ZnO was dissolved in phosphate buffer solution (PBS) of pH 8.0), for which the electrodeposition time was 200 s at -0.9 V. The optimal potential and time for the electrodeposition of ZnO were tested by a comparative study with different potentials (-0.5, -0.7, -0.9, -1.1, -1.3 V) and different times (50, 100, 150, 200, 250, 300 s). -0.9 V and 200 s were appropriate because the multilayer film obtained using 200 s electrodeposition at -0.9 V was mechanically robust and stable during all of the measurements. After being washed with ultrapure water, the electrode was placed in negatively charged dsDNA (1.0 g/L, in 5.0 mmol/L Tris buffer of pH 7.0 containing 5.0 mmol/L Tris-HCl and 0.05 mol/L NaCl) solution for 30 min to adsorb DNA layer on the surface. This adsorption cycle was repeated to the desired number (*n*) to assemble Au/MPA/(ZnO/dsDNA)$_n$ layer-by-layer films on the electrode surface.

MB-loaded Au/MPA/(ZnO/dsDNA)$_n$ film, which was denoted as Au/MPA/(ZnO/dsDNA)$_n$-MB, was constructed by immersing the film electrode into 20 μmol/L MB of B-R buffer solution (pH 6.0, containing 20 mmol/L NaCl) with stirring for 1 h until the loading equilibrium or the steady state was reached. The Au/MPA/(ZnO/dsDNA)$_n$-MB film was then rinsed with B-R buffer, dried with nitrogen stream, and placed in B-R buffer of pH 6.0 for differential pulse voltammetric

1888 *Chin. J. Chem.,* 2009, Vol. 27, No. 10

DU *et al.*

(DPV) scans. The state of Au/MPA/(ZnO/dsDNA)$_n$-MB at this stage was defined as State I. The Au/MPA/(ZnO/dsDNA)$_n$-MB film was then kept in B-R buffer overnight, making most of the loaded MB diffuse out of the films, and DPV was performed in B-R buffer. The state of MPA(ZnO/dsDNA)$_n$-MB at this stage was defined as State II.

For DNA damage experiments, the Au/MPA/(ZnO/dsDNA)$_n$-MB films at State II were incubated in a solution of pH 6.0 consisting of NiSO$_4$ (1.5 mmol/L) and H$_2$O$_2$ (0.5 mol/L) with stirring for a certain time. After being rinsed with ultrapure water, the films were soaked in 20 μmol/L MB solution again for 1 h to reload MB until the steady state was reached. The film electrode was then placed in pH 6.0 B-R buffer for DPV scans. The state of damaged MPA/(ZnO/ dsDNA)$_n$-MB films at this stage was defined as State III. Each measurement was repeated at least three times. Since MB plus light may cause oxidation of guanine in DNA or dsDNA strand breakage under certain conditions, all experiments were performed in dark.

Results and discussion

Electrochemical properties of ZnO/dsDNA multi-layers

Figure 2 shows the CV of electroactive probe [Fe(CN)$_6$]$^{3-/4-}$ at different layer numbers of ZnO/dsDNA membrane. Because dsDNA is negatively charged, (ZnO/dsDNA)$_n$ films will block the electron-transfer of [Fe(CN)$_6$]$^{3-/4-}$ and the redox peak currents should decrease with the growth of the bilayer number (n) gradually, accompanied by the increase of the peak-to-peak separation. Both reduction and oxidation peaks changed linearly with the number of ZnO/dsDNA bilayers (n) up to 5, and then no longer decreased with n any more, indicating that the (ZnO/dsDNA)$_n$ films have been successfully assembled layer-by-layer on the surface of Au/MPA at least when $n < 6$.

The electrochemical impedance spectroscopy can offer information on the impedance changes of the elec-

trode surface during the modification process. Figure 3 shows the results of impedance spectroscopy on nano-ZnO modified electrode and the electrodes with various ZnO/dsDNA bilayer numbers (1—5) in the presence of equimolar 5.0 mmol/L [Fe(CN)$_6$]$^{3-/4-}$ containing 0.1 mol/L KNO$_3$, which were measured at the formal potential of [Fe(CN)$_6$]$^{3-/4-}$. Following the theoretical shape, the impedance spectrum includes a semicircle portion at higher frequencies, which corresponds to the electron transfer limited process, and a linear part characteristic of the lower frequencies to the diffusion-controlled process. From Figure 3, significant differences in the impedance spectra were observed upon the stepwise formation of the multilayers. For the nano-ZnO modified electrode, the impedance spectrum exhibited a visible semicircle. When the ZnO/dsDNA bilayers were assembled, the semicircle portions became larger at the higher frequencies, which indicated that insulating layers on the electrode surface were formed. The diameter of the semicircle part increased significantly with the increase of layer number. The semicircle diameter corresponds to the interfacial electron-transfer resistance R_{et}. In this paper, R_{et} reflects the electron-transfer kinetics of [Fe(CN)$_6$]$^{3-/4-}$ at the electrode interface. The value of R_{et} depends on the dielectric and insulating features at the electrode/electrolyte interface.[18] The increase of the R_{et} value showed the enhanced hindrance effect on the charge transfer of [Fe(CN)$_6$]$^{3-/4-}$. Furthermore, the R_{et} values were proportional to the number of ZnO/dsDNA bilayers, as shown in inset of Figure 3, which illustrated that the multiplayer films were uniformly formed.
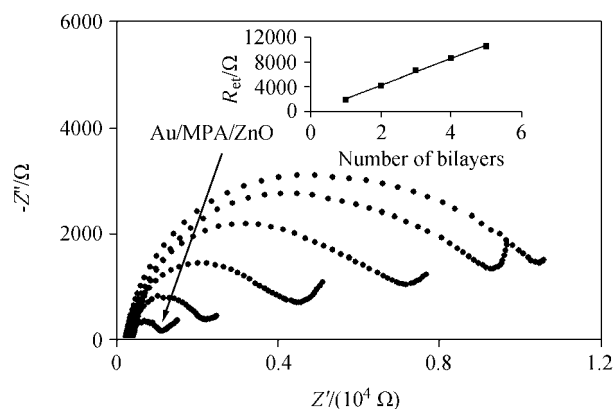
Figure 3 Electrochemical impedance spectroscopies recorded at Au/MPA/ZnO electrode and Au/MPA/(ZnO/dsDNA)$_n$ with increasing number of outmost DNA layers from $n = 1$ to 5 (shown from inside to outside curves) at 0.18 V (vs. Ag/AgCl) in 5.0 mmol/L [Fe(CN)$_6$]$^{3-/4-}$ containing 0.1 mol/L KNO$_3$. Inset: Relationship of the electron-transfer resistance (R_{et}) with the number of ZnO/dsDNA bilayers.

Differential pulse voltammetric measurement of (ZnO/dsDNA)$_5$-MB films

The DPV behavior of Au/MPA/(ZnO/dsDNA)$_5$-MB film in B-R buffer was investigated, and compared with

Figure 2 Cyclic voltammograms of Au/MPA/(ZnO/dsDNA)$_n$ in 1.0 mmol/L K$_4$[Fe(CN)$_6$]/K$_3$[Fe(CN)$_6$] containing 0.1 mol/L KNO$_3$ with increasing number of outmost DNA layers from 1 to 5. Scan rate: 100 mV/s.

DNA damage

Chin. J. Chem., 2009 Vol. 27 No. 10 **1889**

that of Au-MB, Au/MPA-MB or Au/MPA/ZnO-MB film in Figure 4. A well-defined reduction peak was observed at about -0.30 V (curve c), verifying that MB was adsorbed on the ZnO film. Very large DPV response was observed at Au/MPA/(ZnO/dsDNA)$_5$-MB film (curve d). The DPV reduction peak current increased nonlinearly with immersion time in MB solution up to 1 h and then leveled off, achieving the steady state. The main interaction of MB with dsDNA is intercalation of MB into dsDNA base pairs.[19] Thus, MB was mainly loaded in the interior of the films.
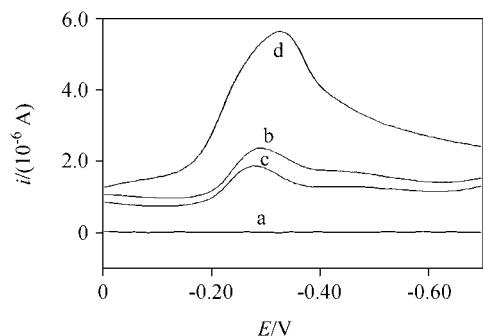
Figure 4 DPV in B-R buffer (pH 6.0) for (a) Au-MB, (b) Au/MPA-MB, (c) Au/MPA/ZnO-MB and (d) Au/MPA/(ZnO/dsDNA)$_5$-MB films.

The loading/release behavior of MB in Au/MPA/(ZnO/dsDNA)$_5$ films is shown in Figure 5. After the fully-loaded Au/MPA/(ZnO/dsDNA)$_5$-MB films (curve a) were immersed into B-R buffer (pH 6.0), the DPV response declined with immersion time, indicating that some MB loaded in the films would be gradually released out of the films and into the B-R buffer. Compared to the initial DPV peak current, about 50% of MB was maintained in the films after 1 h of immersion (State II, curve b). The reduction peak current became smaller and smaller with the increase of time, and eventually reached steady state when the release time of MB from the Au/MPA/(ZnO/dsDNA)$_5$-MB was 6 h (curve c). The plot of the logarithm of the reduction peak currents [$\ln(i_{pc}/\mu A)$] against the release time (t) was straight line for the Au/MPA/(ZnO/dsDNA)$_5$-MB, illustrating that the release of MB obeyed the first-order kinetics according to the following equation.[20]

$$\text{Au/MPA/(ZnO/dsDNA)}_5\text{-MB} \xrightarrow[\text{release}]{k}$$
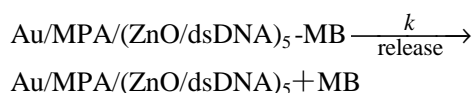
$$\text{Au/MPA/(ZnO/dsDNA)}_5 + \text{MB}$$

Thus, $\ln i = -kt + \text{constant}$

where k is the release rate constant of MB. The linear regression equation was obtained as $\ln i_{pc} = -0.0118t - 1.76$ for the Au/MPA/(ZnO/dsDNA)$_5$-MB. The value of k of MB released from the Au/MPA/(ZnO/dsDNA)$_5$-MB was 1.18×10^{-2} s^{-1} with the half-life period ($t_{1/2}$) of 59 s.
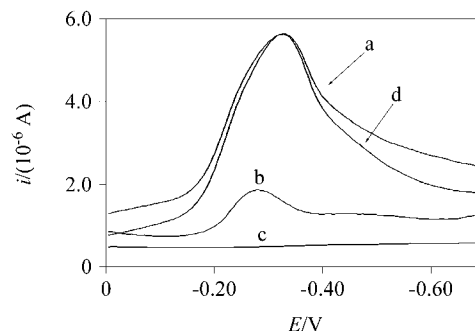
Figure 5 DPV of Au/MPA/(ZnO/dsDNA)$_5$-MB films in B-R buffer (pH 6.0) (a) at State I, at State II after (b) 1 h, (c) 6 h immersion of the films at State I in B-R buffer and (d) at the MB-reloaded films of State II re-immersed in 20 μmol/L MB solution for 1 h.

The DPV curve (curve d) of the MB-reloaded Au/MPA/(ZnO/dsDNA)$_5$ films had nearly identical peak potential and a larger peak height with curve a at State I, suggesting that the loading of MB in Au/MPA/(ZnO/dsDNA)$_5$ films be not perfectly reversible. It was thought that parallel determination for several times could avoid the error caused by instability of the multilayers.

Detection of DNA damage

Figure 6 shows the DPV of Au/MPA/(ZnO/dsDNA)$_5$-MB film in B-R buffer at State III for different incubation time with 1.5 mmol/L NiSO$_4$ solution . As can be seen, the reduction peak current decreased with the prolongation of the incubation time in NiSO$_4$ solution, indicating that the damaged DNA films cannot reload MB to the same level as that of the intact DNA films. With this ''loading/releasing/reloading'' procedure for MB, the DNA damage in the Au/MPA/(ZnO/dsDNA)$_5$ films can be detected sensitively by DPV. For example, compared with that of the intact DNA films (curve c in Figure 5), 10 min of incubation in Ni(II) solution under the present conditions would cause an obvious decrease of DPV reduction peak for the Au/MPA/(ZnO/dsDNA)$_5$-MB films. DPV was preformed in B-R
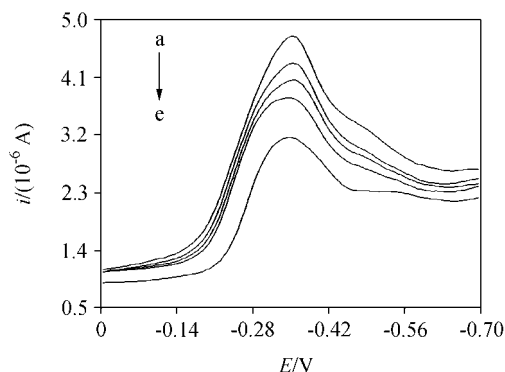
Figure 6 DPV in B-R buffer (pH 6.0) at Au/MPA/(ZnO/dsDNA)$_5$-MB films after incubation in 1.5 mmol/L NiSO$_4$ solution for different time (min): (a) 10, (b) 20, (c) 30, (d) 40, and (e) 50.

buffer instead of in MB solution, in order to distinguish the DPV responses between diffused MB in its solution and incorporated MB in the films. In contrast, for control experiments under the same incubation conditions but without Ni(II), essentially no decrease of DPV response for the films was observed.

Many of the heavy metals may cause DNA damage. A typical route for DNA lesions caused by these heavy metals is through metal catalyzed generation of reactive oxygen species such as hydroxyl free radical in the presence of H_2O_2, the so-called Fenton reaction, for example, Fe^{2+}/H_2O_2 reaction. The Fenton reaction causes DNA cleavage at almost every nucleotide site, leading to base loss, chain breakage, and base oxidation.[21] Many of the base oxidation products can be further oxidized, such as to 8-oxo-7,8-dihydro-2-deoxy-guanosine (8-oxo-dG). In this work, hydroxyl radicals are generated by the reaction of $NiSO_4$ and H_2O_2:

$$NI(II) + H_2O_2 \rightarrow Ni(III) + OH^- + OH\bullet$$

The hydroxyl radical may cause oxidative damage to natural DNA, which would disturb or even completely destroy some of the π-π stack formed by adjacent DNA base pairs in its double helix structure. Since most of MB molecules loaded in the $Au/MPA/(ZnO/dsDNA)_5$ films were intercalated into the duplex structure of dsDNA, the damage of DNA might lead to the release of some MB molecules from the destroyed duplex structure, resulting in the decrease of the corresponding DPV response.

Conclusion

The assembly of alternating nano-ZnO and DNA multilayer films by electrostatic layer-by-layer adsorption has been studied in this article. Cyclic voltammetry and electrochemical impedance spectroscopy were used to characterize the nature of these $(ZnO/dsDNA)_n$ multilayers. The results show that $(ZnO/dsDNA)_n$ multilayer can be successfully fabricated on the 3-mercapto-propionic acid monolayer modified electrode surface. The immobilization amount of DNA was increased with the growth of the ZnO/dsDNA bilayer number (n). On this basis, the $(ZnO/dsDNA)_n$-MB films have been suc-

cessfully used to detect the oxidative damage of natural DNA using electroactive probe MB and DPV technique. The causal factors of DNA damage were the hydroxyl radicals, which were generated by the reaction of $NiSO_4$ with H_2O_2. The loading/release behavior of MB for $(ZnO/dsDNA)_n$-MB films may thus provide a general concept in the study of DNA lesion detection and promising applications to screening new chemicals for their potential genotoxicity.

References

1   Cao, R. J.; Diaz, A.; Cao, R.; Otero, A.; Cea, R. *J. Am. Chem. Soc.* **2007**, *129*, 6927.

2   Wang, B. Z.; Anzai, J. I. *Langmuir* **2007**, *23*, 7378.

3   Shi, Y. T.; Yuan, R.; Chai, Y. Q.; Tang, M. Y.; He, X. L. *J. Eletroanal. Chem.* **2007**, *604*, 9.

4   Decker, G. *Science* **1997**, *277*, 1232.

5   Liu, Y.; Liu, H. Y.; Hu, N. F. *Biophys. Chem.* **2005**, *117*, 27.

6   Zhang, Y.; Hu, N. F. *Electrochem. Commun.* **2007**, *9*, 35.

7   Guo, W.; Hu, N. F. *Biophys. Chem.* **2007**, *129*, 163.

8   Sun, H.; Hu, N. F. *J. Eletroanal. Chem.* **2006**, *588*, 207.

9   Pei, R. J.; Cui, X. Q.; Yang, X. R.; Wang, E. K. *Biomacromolecules* **2001**, *2*, 463.

10 Liu, B.; Zeng, H. C. *J. Am. Chem. Soc.* **2003**, *125*, 4430.

11 Rodriguez, J. A.; Jirsak, T.; Dvorak, J.; Sambasivan, S.; Fischer, D. *J. Phys. Chem. B* **2000**, *104*, 319.

12 Geonel, R. G.; Patricia, S. J.; Jozsef, N.; Imre, D.; David, D. *J. Phys. Chem. B* **2003**, *107*, 12597.

13 Topoglidis, E.; Cass, A. E.; O'Regan, B.; Durrant, J. R. *J. Eletroanal. Chem.* **2001**, *517*, 20.

14 Steenken, S.; Jovanovic, S. V. *J. Am. Chem. Soc.* **1997**, *119*, 617.

15 Mugweru, A.; Rusling, J. F. *Anal. Chem.* **2002**, *74*, 4044.

16 Fojta, M.; Kubicarova, T.; Palecek, E. *Biosens. Bioelectron.* **2000**, *15*, 107.

17 Piedade, J. A.; Oliveira, P. S.; Lopes, M. C.; Oliveira-Brett, A. M. *Anal. Biochem.* **2006**, *355*, 39.

18 Shen, J.; Liu, C. C. *Sensor. Actuat. B-Chem.* **2007**, *120*, 417.

19 Pournaghi-Azar, M. H.; Hejazi, M. S.; Alipour, E. *Anal. Chim. Acta* **2006**, *570*, 144.

20 Zhao, Y. D.; Pang, D. W.; Wang, Z. L.; Cheng, J. K.; Qi, Y. P. *J. Electroanal. Chem.* **1997**, *431*, 203.

21 Cooke, M. S.; Evans, M. D.; Dizdaroglu, M.; Lunec, J. *FASEB J.* **2003**, *17*, 1195.

(E0812234   Pan, B.; Lu, Z.)